

**Ph D. Thesis Title :**

**Coupled effects between mechanical behavior  
and mass transfer phenomena in rock salt**

**Thesis Abstract :**

**INTRODUCTION**

Salt formations are considered as suitable repository media since they are assumed to be impervious to fluids : rock salt has been selected in many countries for underground storage of hydrocarbons, industrial and radioactive waste.

Long term behavior of such facilities depends strongly on both rheological properties and mass transfer properties : salt solubility in water and rock salt permeability. Nowadays, studies dealing with long term safety of storage include two separate approaches : 1) hydrochemical stability studies and 2) mechanical stability studies.

In the first approach, a hydrogeological overview of the disposal site is conducted to identify potential pathways for fluids and radionuclides. Laboratory and *in situ* measurements are also performed in order to study the hydraulic properties (permeability, connected porosity and eventually degree of saturation) in the "near field" of storage. Wieczorek and Rothfuchs (1986) at the Asse Mine (Germany) and Stormont (1991 and 1997) at the Waste Isolation Pilot Plant site (United States) showed that rock salt may have a very low but measurable permeability (in the range of  $10^{-15}$  to  $10^{-21}$  m<sup>2</sup>) related to mechanical damage (nearby excavation). But at present, little is known about the permeability of intact and undisturbed salt far away from the underground facilities, beyond the Disturbed Rock Zone (D.R.Z.) created by mechanical damage.

Following the second approach purely mechanical, analysis of deformations induced by underground excavation is carried out. The influence of time dependent deformation of excavation stability due to the viscoplastic behavior of salt is studied both in laboratory and *in situ* (for instance, Langer, 1981; Munson *et al.*, 1981). In this mechanical analysis, the effect of permeability and fluid percolation are rarely taken into account in spite of laboratory results on the effects of chemically active brine on rock salt deformation (Spiers *et al.*, 1990, Brodsky & Munson, 1991; Schulze, 1991). Physico-chemical reactions between brine and grain boundaries or microcracks lead to a weakening of salt mechanical properties. These effects and other geochemical effects on transport properties of salt are not considered in the long term safety analysis of

storage certainly due to the lack of a theoretical framework allowing coupled effects analysis (e.g. long term thermo-hydro-chemico-mechanical behavior of salt).

The main objective of the thesis was to reexamine the hypotheses of this uncoupled approaches for long term safety assessment of storage in rock salt. The thesis focused on the following questions :

- in which conditions, rock salt is permeable to fluids (gas, brine, .. ) ?
- if so, what are the processes governing a fluid percolation in very low porous media such as salt formations ? (Darcy's law ? what is the role of geochemical interactions ?)
- What are the effects of a very low percolation on the mechanical stability of storage ?
- How will the thermo-mechanical loading induced by an excavation or radioactive wastes influence the permeability of the rock mass and consequently, the long term evolution of storage ?

To answer to these questions, a field experiment at the Mines de Potasse d'Alsace (M.D.P.A., France) which required preliminary theoretical and experimental studies for the conception, performance and interpretation of the test, was performed. This experiment was completed by laboratory triaxial tests carried out on samples taken from the same site. The whole experimental results are discussed in the first part of the thesis.

In the second part, a theoretical macroscopic framework is presented, considering the rock salt as a porous medium in which a chemical reaction occurs between the fluids and the matrix.

The third part is a contribution to the safety analysis of underground disposals in saline formations. In this framework, the so-called "Healing" process leading to closure of the discontinuities (microcracks and grain boundaries) is discussed. Then, a preliminary study of the effect of an extremely low permeability on the long term evolution of a storage is proposed with the help of a model with a simple geometry based on the *in situ* experimental results.

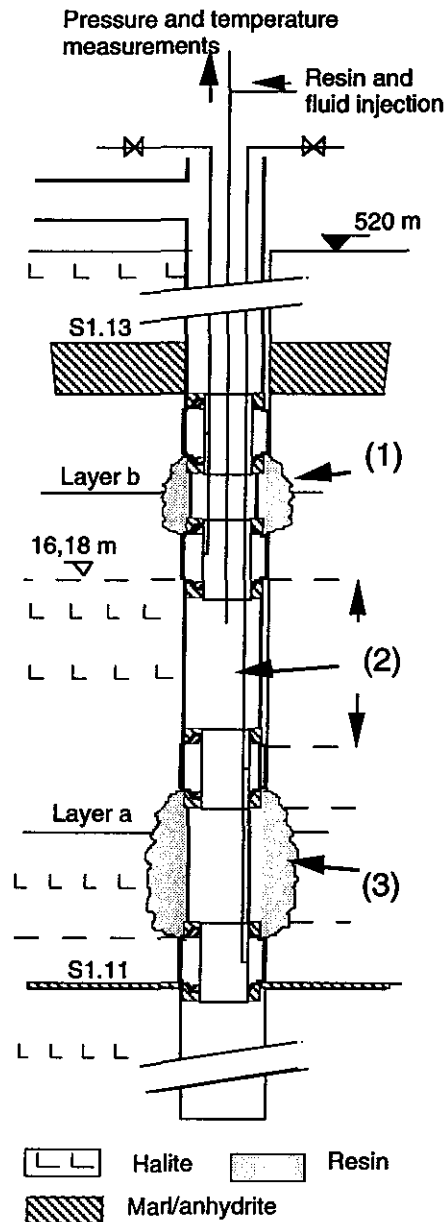
## **IN SITU ROCK SALT PERMEABILITY MEASUREMENT**

A review of hydro-mechanical behavior of rock salt show that two main mechanical phenomena are involved in permeability evolution : (a) deviatoric loading leads to a microfracturing and dilatation of grain boundaries, (b) hydrostatic loading induces an instantaneous elastic closure of the existing microcracks and a continuous "healing" of the discontinuities (microcracks and grains boundaries).

The first phenomenon explains why the zone surrounding an underground storage in salt has reduced hydrogeological and mechanical properties (Stormont,

1991). But little is known if the second phenomenon can reestablish the initial permeability.

In order to study the conditions in which rock salt is really impervious, an *in situ* test experiment was performed in the Amelie mine belonging to the Mines de Potasse d'Alsace (M.D.P.A., France). A vertical borehole, 20 m long, was drilled from an excavated depression to access to the S1 bed, very low in insolubles (figure 1). The selected salt bed is approximately one metre thick and is located 16 metres away from the gallery floor. This distance was assumed to be sufficient to put the tested zone beyond the area disturbed by mining.



- (1) Upper leak-tight chamber
- (2) Test chamber
- (3) Lower leak-tight chamber

Figure 1. Borehole Equipment

## 1. EXPERIMENTAL PROCEDURE

A preliminary study on thermo-hydro-chemico-mechanical processes in salt showed that the measurements can be disturbed by various effects : solution-crystallization associated with brine percolation, thermal expansion and creep (Cosenza and Ghoreychi, 1993). To control them, the following recommendations were made and adopted : (a) tests with constant pressure steps, (b) thermal regulation of the test. Moreover, a special set-up was designed and the principal components (packer, resin sealant, injection system...) were tested in the laboratory prior to the field test (figure 2).

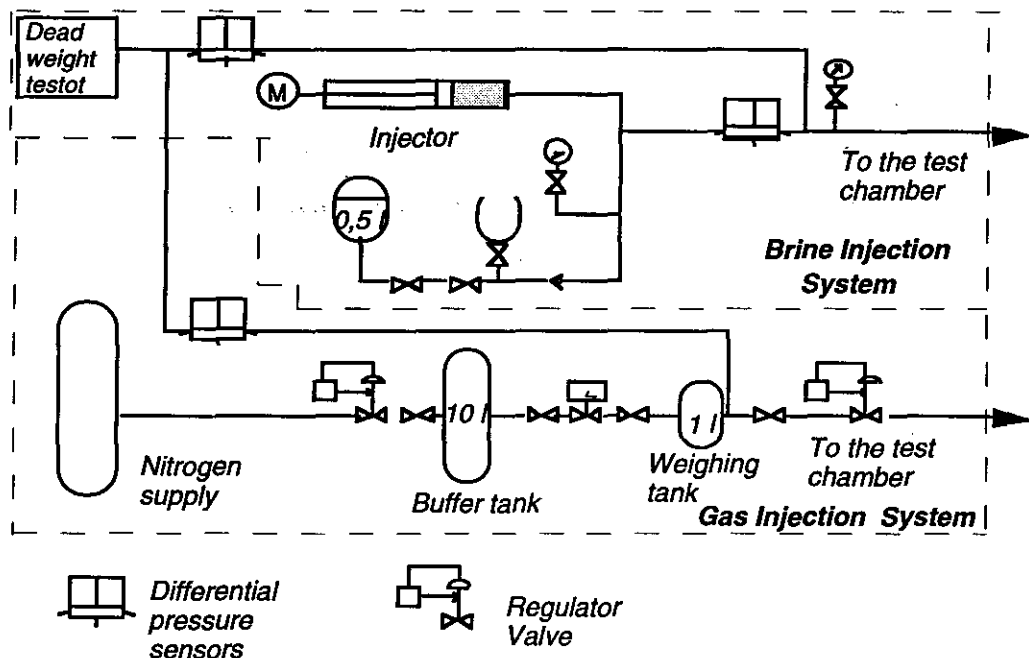


Figure 2. Fluid Injection Set-Up (Gas and Brine)

A special heat regulation system was developed to keep the temperature of the injected fluid constant close to that of the rock mass.

The set-up was ready for use in July 1994. The *in situ* experiment was conducted in three main phases.

First, a preliminary gas test was performed with nitrogen to check the leak-tightness of the set-up and to measure the initial rock mass permeability to gas. This experiment went on as follows: the test chamber was subjected to a fluid pressure,  $P_g$ , which then subsided as fluid leaked into the formation. When the pressure reached a lower limit of  $P_g - \Delta P$  ( $\Delta P$  negligible with respect to  $P_g$ ), a predetermined quantity of gas was injected into the chamber. The gas pressure inside the chamber during the test was therefore considered to be constant and equal to  $P_g$  with a small deviation  $\Delta P$ . After this first gas injection phase at a pressure level of 2 MPa during 18 days, two other similar tests were performed with gas and pressures of 4 and 6 MPa, during 26 and 16 days respectively.

In the second phase, which took place after the pore pressure had been allowed to dissipate for one week, the chamber was subjected to a brine pressure of 2, 4 and 6 MPa for 27, 19 and 34 days respectively. The pressure was maintained at the requested level through a *continuous* injection of brine. In the third and final phase, after the brine seepage, the chamber was again subjected to a gas pressure of 6 MPa for 15 days.

## 2. RESULTS AND INTERPRETATION

### 1. Gas test

The injected mass of nitrogen during the first phase is plotted on the figure 3. Two particular features are observed : whether the chamber pressure is 4 or 6 MPa, the average mass flow rate in the beginning of each injection is still equal to about 4 g/day and does not increase as a function of the chamber pressure as expected. This suggests that Darcy's law is not valid for a gas flow in salt. Furthermore, no significant transient state is observed.

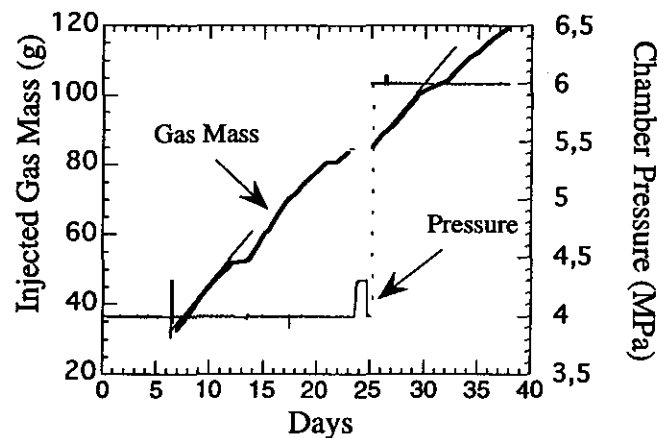


Figure 3. Injected Gas Mass During Two Pressure Steps, 4 and 6 MPa.

The evolution of chamber pressure during the third phase after brine injection shows that gas migration in salt was reduced considerably. After 14 days, the average gas mass flow rate was divided by a factor of ten. This result confirms the effect of capillary pressure due to the small size of the pores in salt.

### *Discussion on flow mechanism*

Let us consider first, a miscible displacement of dissolved gas in liquid. Supposing a flow in a steady state, the dissolved mass of gas diffused through the liquid phase, after

equilibrium, can be estimated and compared with the experimental values. The calculation shows that only a very small quantity of gas can be dissolved and migrate in brine (some milligrams/day) : miscible displacement can be neglected. Gas migration has to be considered with respect to a two-phase immiscible flow.

Therefore, one can imagine that at least two fluid phases are present in the pores and are separated by an interface. In a porous medium, with a small pore size about  $10^{-9}$  m such as rock salt, the interface is subjected to a surface force resulting from a difference of pressure across the interface. This so called capillary pressure was estimated to be theoretically in the range of one to a few hundred MPa (Cosenza and Ghoreychi, 1993). But the results of the third injection phase suggest that capillary pressure does not exceed about one MPa.

Considering a multiphase flow of immiscible fluids, two simple models are given :

*a- porous medium saturated with gas;*

*b- mobile boundary between injected gas and initial brine.*

Both simple models of multiphase flow of nonmiscible fluids, neglecting capillary pressure do not fit the experimental data. Consequently, gas percolation does not obey Darcy's law if the medium is assumed to be saturated.

A nonuniform distribution of capillary pressure and complex microscopic mechanisms, like Klíngenberg's effect ("wall slips" in the pore network) seem to play an important role.

For gas flow, the lack of information concerning the initial conditions (saturation state, initial capillary pressure) and the boundary conditions away from the borehole did not allow us to clearly identify the main flow mechanism.

## **2. Brine test**

The evolution of the percolated brine volume is plotted on the figure 4.

In order to check the validity of Darcy's law, the measurements were analyzed with a numerical model on the basis of the following assumptions : rock salt is saturated with brine, the tested volume is a cylinder.

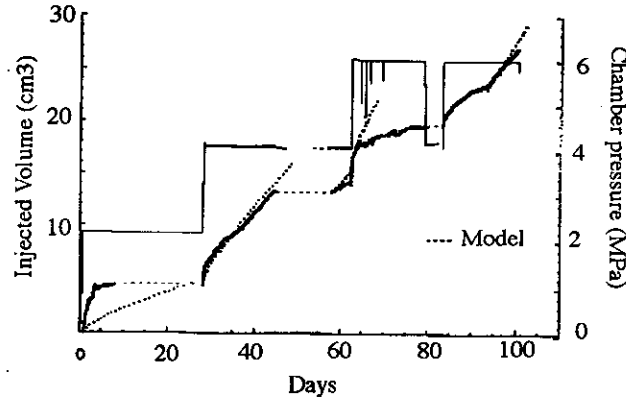


Figure 4. Injected Brine Volume During Three Pressure Steps, 2, 4 and 6 MPa (the first 6 MPa pressure step is not taken into account due to thermo-regulation problems).

The first assumption can be justified only for the second pressure step. The first pressure step at 2 MPa was influenced by the previous gas injections, since the rock mass was not initially saturated with brine. The second assumption was verified by comparing the penetration distance of brine (on the order of 15 cm) and the chamber height (75 cm).

Using previous assumptions, rock salt permeability can be calculated by solving the following diffusion equation of pore pressure in a poro-viscoplastic rock mass :

$$\frac{k}{\eta} \nabla^2 P = \frac{1}{M} \frac{\partial P}{\partial t} + b \frac{\partial e}{\partial t} + \underbrace{\frac{\partial \phi^{VP}}{\partial t} - b \frac{\partial e^{VP}}{\partial t}}_{\text{contribution of viscoplasticity}} \quad (1)$$

P: pore pressure (Pa); k : intrinsic permeability ( $\text{m}^2$ );  $\eta$  : dynamic viscosity (Pa.s);  $\nabla^2$  : Laplace operator; M : Biot's modulus (Pa); b: Biot's coefficient; e : total volumetric strain ;  $\phi^{VP}$  : irreversible porosity;  $e^{VP}$  : irreversible volumetric strain.

In equation (1), two transient terms are due to viscoplastic flow. The first term corresponds to the change in irreversible (viscoplastic) porosity :  $\phi^{VP}$ . The second term is related to irreversible volumetric strain  $e^{VP}$ . No assumption on rock salt behavior was made.

For undisturbed salt, viscoplastic strains are associated, at a microscopic scale, with dislocation movements (glide and climb), grain boundary/volume diffusion (Langer, 1981; Munson and Dawson, 1981) or dissolution-crystallization processes in the presence of brine (Spiers *et al.*, 1990). These phenomena do not lead to any significant volumetric strain, therefore equation (1) can be simplified as follows :

$$\frac{k}{\eta} \nabla^2 P = \frac{1}{M} \frac{\partial P}{\partial t} + b \frac{\partial e}{\partial t} \quad (2)$$

Keeping constant hydraulic boundary conditions with no displacement away from the borehole, equation (13) can be reduced to (see for instance, Coussy, 1995) :

$$k_{fl} \nabla^2 P = \frac{\partial P}{\partial t} \quad (3)$$

$k_{fl}$  : hydraulic diffusivity defined by :

$$k_{fl} = \frac{k}{\eta} \frac{3K_o + 4\mu}{3K + 4\mu} \left( \frac{b - \phi}{K^s} + \frac{\phi}{K^{fl}} \right)^{-1}$$

$k$  : intrinsic permeability;  $\eta$  : dynamic viscosity ( $1.7 \cdot 10^3$  Pa.s at 25 °C ATG, 1986);  $b$  : Biot's coefficient (0.1; Mc Tighe, 1986);  $\phi$  : porosity (0.1 %; Thorel and Ghoreychi, 1991);  $K^s$  and  $K^{fl}$  : modulus of compressibility of solid and fluid respectively ( $K^s=25$  GPa for salt,  $K^{fl}=3.7$  GPa for brine, ATG, 1986);  $K_o$  : drained bulk modulus (22.5 GPa calculated from  $K^s$  and  $b$ );  $K$  : undrained bulk modulus (24.4 GPa calculated from  $K_o$ ,  $\phi$ ,  $K^s$ ,  $K^{fl}$  and  $b$ , Coussy, 1991).

Considering an isothermal flow, the model results and the measurements are compared for 4 and 6 pressure steps (Fig. 4). Figure 4 shows that by solving equation (3) numerically with respect to the loading history, the best curve fitting is obtained for an intrinsic permeability of  $2 \cdot 10^{-21}$  m<sup>2</sup> and an initial pore pressure  $P_o$  of 1 MPa. Therefore, Darcy's law seems to apply to brine percolation, even if the permeability is very low, since the fitting is satisfactory for the whole history of injection pressure.

Moreover, with transient modeling, it is possible to estimate the extent of the zone influenced by the hydraulic flow. It can be characterized by a parameter, called "radius of influence", which is defined arbitrarily as the distance from the borehole wall where the value  $P_1 + \Delta P_{max}/10 = P_1 + (P_1 - P_o)/10$  ( $P_1$  : chamber pressure and  $P_o$  : initial pore pressure) is reached. This calculation yields 2 m, which is greater than the Representative Elementary Volume of the porous salt and also greater than the extent of the zone disturbed by drilling.

The results of the transient modeling suggest that nonlinear effects associated with permeability play a minor role or compensate each other. These effects are :

- (1) variation in effective stress,
- (2) change in the chemical equilibrium of brine resulting from pressure changes, inducing dissolution-crystallization,
- (3) rock damage during drilling due to the generation of high deviatoric stresses,



### 3. Impact of rock salt disturbance around the borehole

Since mechanical drilling disturbs the rock salt, the sensitivity of the measurements to the flow through the damaged rock around the borehole was investigated. It was felt necessary to verify that the brine tests were long enough to allow the brine percolation in the undisturbed salt.

A simple method of predicting the development of damage in a rock salt is to compare the stresses on the excavation wall with a damage criterion obtained by laboratory tests (Thorel et Ghoreychi, 1993).

An experimental work based on compression and extension triaxial tests was carried out to define a damage criterion for rock salt. The experiments were performed first in dry conditions, using a tight jacket (Thorel, 1994) and then in wet conditions, without jacket, in order to allow the confining fluid (brine or oil) to percolate in the sample (Figure 5).

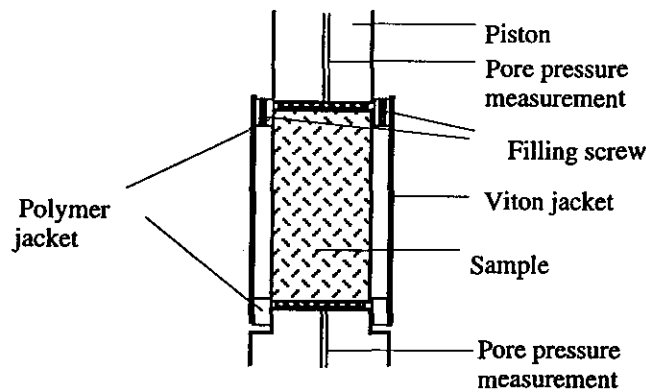


Figure 5 : Triaxial device for wet condition tests

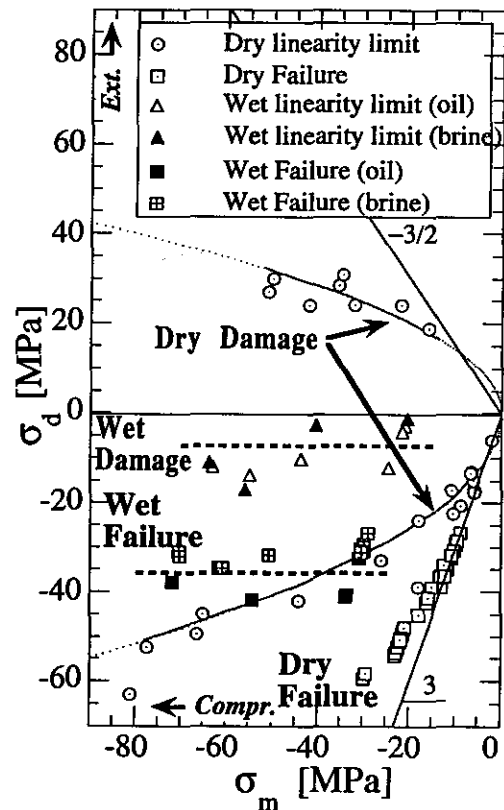


Figure 6: Failure and Dilatancy Criteria in Stress Plane in Dry and Wet Conditions.

In triaxial wet tests, confining fluid is injected with the help of a filling screw between a viton jacket and the sample. Pore pressure is measured by two pressure transducers.

Three values of confining pressure were applied : 20, 40 and 60 MPa. The main results are the following :

- a- Whatever the mean stress and the confining fluid are, the failure remains brittle. This is not the case when the samples are submitted to the same value of confining pressure, in dry condition (with jacket). This phenomenon is attributed to the fluid percolation through the sample, even in a small quantity. The measured maximum deviatoric stress is in the range of 27-42 MPa (Figure 7).
- b- The measured pore pressure values are very small regarding the applied confining pressure, except in the post failure domain, where the cracks are well developed and lead to a significant increase of porosity and permeability.
- c- The value of maximum strength does not depend, in a significant way, on mean stress.
- d- Even in presence of microcracks, Young's modulus is not changed significantly.
- e- Confining fluid has a significant effect on the strength of material (Fig. 6). Average of maximum strength is 37 MPa for the tests performed with brine and 30 MPa for those using oil.

In order to check the damage possibility, two different behaviors were analysed for the rock mass, always in an isothermal condition and assuming a cylindrical symmetry :

(a) A poro-elastic behavior maximizing the damage risk since viscoplastic flow of salt leads to the relaxation of deviatoric stresses on the borehole wall (Kazan and Ghoreychi, 1996).

(b) A steady-state poro-viscoplastic behavior (stress relaxation rate tending to zero). By assuming the existence of an asymptotic state of stress (which is a reasonable assumption see Pouya, 1991), in thermal and hydraulic steady states, the limits of deviatoric stress and mean stress on the borehole wall can then be calculated (Pouya, 1991; Kazan and Ghoreychi, 1996) (see Table 1).

The stress fields calculated in Table 1 are compared with the damage criteria obtained for the MDPA salt in dry and wet conditions (Fig.7).

Table 1. Relationships Between Mean Stress and Deviatoric Stress for Two Types of Behaviors : Poro-elastic and Poro-viscoplastic for Different Pressure Steps,  $P_0$  initial pore pressure (=1 MPa) ;  $\sigma_0$  : initial stress (= 10 MPa);  $n=3$  (creep law exponent) ;  $\nu_0=0.3$ ;  $b=0.1$ .

	Relations	$P_1=0$ MPa	$P_1=2$ MPa	$P_1=6$ MPa
<b>Poro-elasticity</b>				
Mean stress $\sigma_m = \frac{1}{3} tr \underline{\underline{\sigma}}$	$\sigma_m = \sigma_0 + \frac{2}{3} b \frac{1-2\nu_0}{1-\nu_0} (P_1 - P_0)$	10	10.0	10.2
Deviatoric stress $\sigma_d = \sigma_\theta - \sigma_r$	$\sigma_d = 2(\sigma_0 - P_1) - b \frac{1-2\nu_0}{1-\nu_0} (P_1 - P_0)$	20	15.9	7.7
<b>Poro-viscoplasticity</b>				
Mean stress	$\sigma_m = \frac{1}{3} (2P_1 + \sigma_0) - \frac{2}{3} [\nu_0(1-n) - 1] \left( \frac{-\sigma_0 + P_1}{n} \right) + \frac{1-2\nu_0}{3} b (P_1 - P_0)$	4.2	5.4	8.6
Deviatoric stress	$\sigma_d = \frac{2}{n} (\sigma_0 - P_1)$	6.7	5.3	2.7

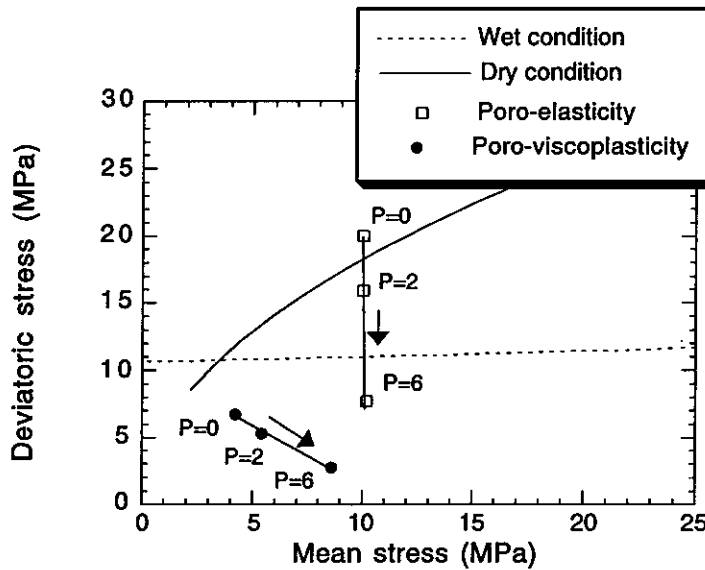


Figure 7. Stress state on the borehole wall compared with salt damage criteria.

Figure 7 shows that the stress state corresponding to a zero pressure level, calculated by assuming instantaneous drilling of the borehole and elastic behavior of the rock mass, is situated above the dry damage criterion. Nevertheless, the state corresponding to the pressure value of 6 MPa is slightly below the wet damage

criterion. Regarding the discrepancy of the laboratory results and the uncertainty on the initial stress, it can be concluded that the eventual damage (if it does exist) is small and localized in the vicinity of the chamber wall.

When the fluid is not present in the borehole (zero pressure on the wall), a numerical calculation was made using an elastoplastic model (Thorel et Ghoreychi, 1993). The results show that the damaged zone surrounding the borehole does not extend beyond a distance of 1.5 borehole radius. Regarding the radius of the chamber (7.3 cm), the calculated damaged zone is 4 cm thick. The radius of the damaged zone is to be compared with that of the brine penetration distance, estimated to be 15 cm. The factor of 3.75 between these two values suggests that the measured permeability value cannot be attributed to the salt damage only.

When a fluid pressure is applied to the borehole wall, the extent of damaged zone can easily be estimated by assuming that :

(a) the damage threshold is not dependent on average stress, Tresca's criterion can be assumed :

$$F = \text{Sup}_{i,j} |\sigma_i - \sigma_j| - 2C$$

$\sigma_i$  and  $\sigma_j$  : extrema principal stresses ;  $C$  : cohesion equal to 5 MPa, according to figure 7.

(b) there is a great difference between the permeabilities of damaged and undisturbed rock salt, and also, the extent of the damaged zone is small. In addition, pore pressure evolution in the damaged zone is neglected.

The calculation of the radius of the damaged rock zone (formally a plastic radius) may be expressed as follows :

$$\ln \frac{R}{r_o} = \frac{1}{2C} \left[ -C + \sigma_o - P_1 + b \left( \frac{1-2\nu_o}{1-\nu_o} \right) \left( \frac{P_1 - P_o}{2} \right) \right] \quad (15)$$

$r_o$  : radius of borehole;  $P_o$  : initial pore pressure,  $P_1$  : fluid pressure on the borehole wall,  $\nu_o$  : drained Poisson's ratio,  $b$  : Biot's ratio.

This equation shows clearly that the higher the pressure applied to the wall, the smaller the extent of the damaged zone : the pressure on the borehole wall functions as a liner. Using the values given in Table 5, a numerical calculation gives a value  $R/r_o$  of 1.3 when the fluid pressure on the wall is 2 MPa (minimum pressure on the wall). Regarding the radius of the chamber (7.3 cm), then the damaged zone extent is 2 cm. Again this value is to be compared with the penetration distance of 15 cm. The factor of 7.5 between these two values confirms once more that the role of damage is limited.

## THEORETICAL FRAMEWORK OF COUPLED EFFECTS IN SALT

The developed framework is based on the macroscopic description of the coupled phenomena obeying to the principles of Thermodynamics of Open Continuum Media (Biot, 1941; Coussy, 1991).

This approach allows to set up a general constitutive laws for the reactive porous media, following three steps :

**1<sup>st</sup> Step :** An Equivalent Continuum Medium is defined using the Representative Elementary Volume.

**2<sup>nd</sup> Step :** Each element of the Equivalent Continuum Medium is an elementary system, the thermodynamical equilibrium of which is defined by the following state variables:  $\underline{\underline{\varepsilon}}$  : elastic strain tensor; T : temperature; m : liquid mass supply and  $\underline{\underline{\xi}}$  : mass exchange between solid phase and liquid phase normalized by the initial volume.

**3<sup>rd</sup> Step :** The fundamental state equations linking the state variables are obtained by writing the first and second principles of thermodynamics. For instance, the mechanical state equation is written as follows :

$$\underline{\underline{\varepsilon}} = \frac{1+\nu_o}{E_o} (\underline{\underline{\sigma}} - \sigma_o \underline{\underline{1}}) - \frac{\nu_o}{E_o} \text{tr}(\underline{\underline{\sigma}} - \sigma_o \underline{\underline{1}}) \underline{\underline{1}} + \frac{b}{K_o} \frac{P - P_o}{3} \underline{\underline{1}} + \alpha_o^t (T - T_o) \underline{\underline{1}} + \alpha_o^c \underline{\underline{\xi}}$$

$\underline{\underline{\varepsilon}}$  : elastic strain tensor;  $E_o$  : drained Young's modulus;  $\nu_o$  : drained Poisson's coefficient;  $\underline{\underline{\sigma}}$  : total stress tensor;  $\sigma_o$  : initial stress; b : Biot's coefficient ;  $K_o$  : drained bulk modulus; P : pore pressure;  $P_o$  : initial pore pressure; T: temperature;  $T_o$  : initial temperature;  $\alpha_o^t$  : thermal drained linear expansion.

A chemical strain associated with the chemical reaction is involved :

$$\underline{\underline{\varepsilon}}^{ch} = \alpha_o^c \underline{\underline{\xi}}$$

$\alpha_o^c$  : chemical drained linear expansion (obtained if  $P=P_o$ ).

Using diffusion laws (Darcy's law; Fourier's law, Fick's law) and the different balance equations (brine mass, salt mass in solution and energy), a system of 4 equations (3 scalar and 1 vectorial) with 4 unknowns ( $\underline{\underline{u}}$  : displacement; P: pore pressure; T : temperature; C : salt concentration ) is obtained :

Hydraulic equation :

$$\begin{aligned} \frac{1}{M} \dot{P} + b \dot{\epsilon} - \frac{(\rho_o^{fl})^2 L}{M T_o} \dot{T} + (-1 + \frac{\alpha_o^c K_o}{M b}) \phi_o \frac{S}{V} K_c (C_s - C) \\ = \text{Div}(\frac{k}{\eta} \underline{\text{grad}} P + \frac{K_c^p}{\rho_o^{fl}} \underline{\text{grad}} C + \frac{K_t^p}{\rho_o^{fl}} \underline{\text{grad}} T) \end{aligned}$$

Solute mass equation :

$$\begin{aligned} \phi_o (1 + C_o \alpha_{fl}^c) \dot{C} + C_o b \dot{\epsilon} + C_o (\frac{b - \phi_o}{K_o}) \dot{P} + C_o (\phi_o \alpha_{fl}^t - \alpha_o^t) \dot{T} \\ = \text{Div}(\underline{D} \underline{\text{grad}} C - \underbrace{\underline{C} \underline{U}}_{\text{convective term}} + K_t^c \underline{\text{grad}} T) + (1 + C_o b \alpha_o^c) \phi_o \frac{S}{V} K_c (C_s - C) \end{aligned}$$

Thermal equation :

$$\begin{aligned} (m_o C_E + \frac{\rho_o^{fl} L^2}{M T_o}) \dot{T} + (\alpha K T - L \rho_o^{fl} b) \dot{\epsilon} - \frac{\rho_o^{fl} L}{M} \dot{P} + \frac{\mathfrak{R}}{T_o} \phi_o \frac{S}{V} K_c (C_s - C) \\ = \text{Div}(\lambda \underline{\text{grad}} T + K_c^t \underline{\text{grad}} C + K_c^t \underline{\text{grad}} T - \rho_o^{fl} c^{fl} \frac{k}{\eta} \underline{\text{grad}} P) \end{aligned}$$

Navier (mechanical) equations :

$$(K_o + \frac{4}{3} \mu) \underline{\text{grad}}(\text{Div} \underline{u}) - \mu \text{curl}(\text{curl} \underline{u}) - \underline{b} \underline{\text{grad}} \dot{P} - 3 \alpha_o^t K_o \underline{\text{grad}} \dot{T} - 3 \alpha_o^c K_o \underline{\text{grad}}(\phi_o \frac{S}{V} K_c (C_s - C)) + \underline{m} \underline{F} = 0$$

Nomenclature :

$\alpha_o^t$  : thermal drained linear expansion;  
 $\alpha_o^c$  : chemical drained linear expansion;  
 $\alpha_{fl}^c$  : brine chemical linear expansion;  
 $\alpha^t$  : thermal undrained linear expansion;  
 $\alpha^c$  : chemical undrained linear expansion;  
 $b$  : Biot's coefficient ;  
 $C_s - C$  : volumetric undersaturation ;  
 $c^{fl}$  : brine heat capacity;  
 $\underline{\epsilon}$  : elastic strain tensor;  
 $\epsilon$  : trace of tensor  $\underline{\epsilon}$ ;  
 $\phi$  : porosity;  
 $\eta$  : dynamic viscosity ;  
 $k$  : intrinsic permeability ;  
 $K_o$  : drained bulk modulus ;  
 $D$  : diffusion coefficient of salt in brine;  
 $\text{Div}$  : divergence operator;  
 $\underline{\text{grad}}$  : gradient operator;

$K_c$  : dissolution rate;  
 $K_b^a$  : coupling coefficient of the term  $\underline{\text{grad}} b$  related to conduction law on state variable a;  
 $C_E$  : heat capacity at constant volumetric strain;  
 $\lambda$  : thermal conductivity ;  
 $L$  : specific latent heat per unit value of fluid mass supply;  
 $\mu$  : shear modulus;  
 $m$  : brine mass supply;  
 $M$  : Biot's modulus;  
 $P$  : pore pressure;  
 $\rho^{fl}$  : brine density;  
 $\mathfrak{R}$  : undrained reaction enthalpy;  
 $S/V$  : ratio of surface area of the mineral divided by volume of the solution;  
 $\sigma_o$  : initial stress;  
 $T$  : temperature;  
 $\text{curl}$  : curl operator;

Subscript o indicates the initial state.

These equations can provide a basis for a finite element (or finite difference) computer program to handle coupled problems in the framework of safety analysis of storage.

To discuss the conditions for which one or several processes can be uncoupled, a monodimensional evolution was considered and the transport dimensionless equations were written. The dimensionless analysis showed that the coefficients related to the kinetics of the chemical reaction impose a chemical equilibrium ( $C=C_s$ ).

For rock salt, the terms related to the pore pressure (convection terms) have no effect on the salt mass transfer and the heat transfer due to the very low permeability of the medium.

## CONTRIBUTION TO THE SAFETY ANALYSIS OF UNDERGROUND DISPOSALS IN SALINE FORMATIONS

### 1. PERMEABILITY EVOLUTION OF ROCK SALT UNDER MECHANO-CHEMICAL STRESSES

The previous theoretical framework is used to discuss two phenomena involved in geochemical interactions leading to the changes in transport properties : (1) dissolution/crystallisation in microcracks due to brine solubility changes (2) local chemical potential gradient induced by local normal stress gradient.

In the first case, a simple permeability model, based on isotropic distribution of microcracks is used. Microcracks are considered to be the planes characterized by three microstructural parameters : average microcrack spacing, two mean characteristic lengths (length and half-aperture).

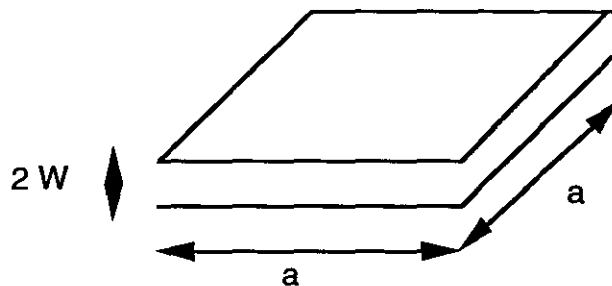


Figure 8. simplified model of microcracks

Brine solubility evolution induced by diffusion of pore pressure or diffusion of temperature is supposed to change the mean half-aperture.

On the basis of a previous theoretical study, the following system of equations with pore pressure  $P$  and temperature  $T$  as the unknowns, were written :

$$\left(\frac{1}{M} + \frac{b^2}{K + 4/3\mu}\right) \frac{\partial P}{\partial t} + (-3\alpha_m + \frac{3aK}{K + 4/3\mu}) \frac{\partial T}{\partial t} + \frac{\partial \phi^{chim}}{\partial t} = \text{Div} \left[ \frac{k(\phi^{chim})}{\eta} \underline{\text{grad}} P \right]$$

$$(\rho C) \frac{\partial T}{\partial t} = \text{Div} [ \lambda_T \underline{\text{grad}} T ]$$

M : Biot's modulus; b: Biot's coefficient; K : undrained bulk modulus;  $\mu$  : shear modulus;  $\alpha$  : thermal undrained expansion;  $\alpha_m$  : thermal expansion of the mixture; k : intrinsic permeability;  $\eta$  : dynamic viscosity;  $\rho$  : salt density; C heat capacity;  $\lambda_T$  : thermal conductivity;

This system was completed by the laws governing the induced chemical porosity change  $\phi^{ch}$  and the induced chemical permeability change  $k^{chim}$ . These laws are obtained through the permeability model, and by using an experimental equation linking salt solubility and brine state variables (temperature and pressure).

The results of coupled numerical calculations on a cylindrical cavity show that the dissolution-crystallization effect does not change the order of magnitude of the initial transport properties and remains much smaller than the influence of thermal loading and that of effective pressure (Figure 9).

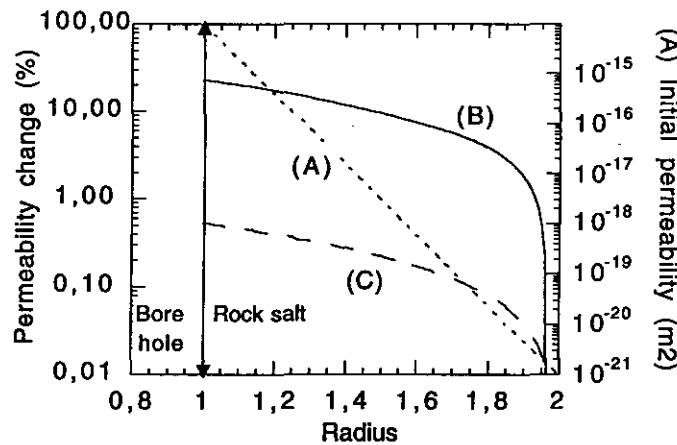


Figure 9. Permeability changes due to cristallization (C) and thermo-mechanical loading (B) (both normalized by initial permeability) versus normalized distance from borehole wall Right : logarithm of initial permeability (A), close to the experimental data obtained at the W.I.P.P. site (Stormont, 1991). Boundary conditions are  $P_0=P_1=12$  MPa;  $T_1=10^\circ\text{C}$  at borehole wall ( $R=1$ , if R is a normalized distance from borehole wall);  $T_0=50^\circ\text{C}$  (initial temperature and temperature at the boundary of disturbed zone  $R=2$ ).

In the second case, a local chemical potential gradient induced by local normal stress gradient is supposed to produce a local mass transfer from grain boundaries towards the



microcracks, leading to "healing" of the latter (figure 10). At a microscale, the driving force is a chemical potential difference related to normal stress as follows (Ollivella *et al.*, 1992) :

$$\delta\mu_s = \phi(\sigma - P)V_m$$

$\phi$  : porosity;  $\sigma$  : applied hydrostatic pressure;  $P$  : pore pressure;  $V_m$  : molar volume.

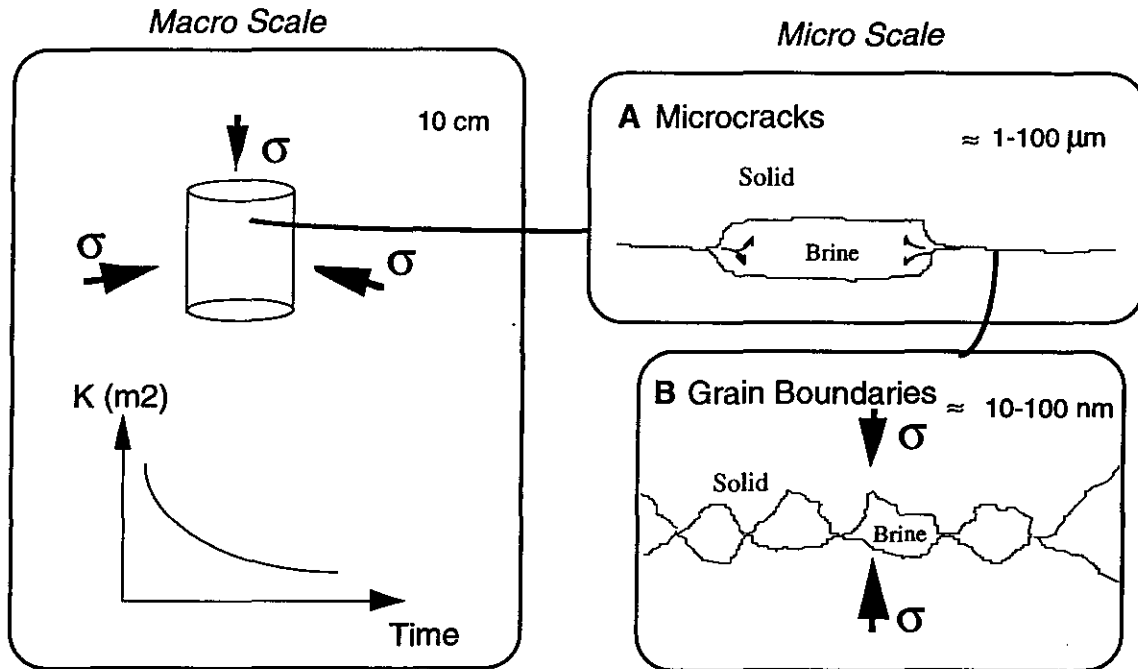


Figure 10. Two spatial scales to be considered in the "healing" process.

The results of the calculations made by using the permeability model mentioned above are in agreement with those of Peach [1991] (figure 11), and suggest that mechano-chemical coupled effect associated with viscoplastic deformation of grains can explain the extremely low permeability of rock salt at a geological time scale.

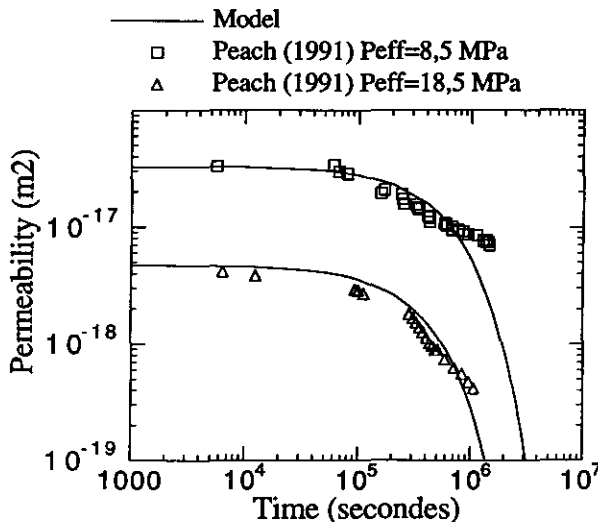


Figure 11. Comparison between experimental data and model .  $P_{eff} = \sigma - P_f = 8,5$  MPa; confining pressure  $\sigma = 10$  MPa and pore pressure  $P_f = 1,5$  MPa.  $P_{eff} = \sigma - P_f = 18,5$  MPa; confining pressure  $\sigma = 20$  MPa and pore pressure  $P_f = 1,5$  MPa.

## 2. EFFECT OF VERY LOW PERMEABILITY OF SALT ON THE LONG TERM EVOLUTION OF A STORAGE

To study the effect of very low permeability of salt on the long-term evolution of a storage, a simple calculation was made on a spherical cavern in a steady state evolution. Rock salt is considered as a poro-viscoplastic medium obeying Norton-Hoff's law based on a steady state creep constitutive model.

In these conditions, equilibrium pressure  $P_1$  in the cavern satisfies the following equations :

- fluid mass balance in the cavern ;
- pore pressure diffusion in the rock mass;

From these equations, we obtained a non linear equation with  $P_1$  as the unknown :

(if permeability  $k=\text{constant}$  in the rock mass)

$$\frac{1}{2} \eta_s(T) \left( \frac{3}{n} \right)^n \left( \frac{\sigma_0 - P_1}{2\sigma_n} \right)^n = \frac{k}{\eta} \frac{P_1 - P_0}{r_0}$$

$\eta_s(T)$  : salt fluidity, function of temperature ;  $n$  : exponent of viscoplastic criterion ;  $\sigma_0$  : initial hydrostatic stress;  $\sigma_n=1\text{MPa}$ ;  $k$  : intrinsic permeability;  $P_0$  : initial pore pressure;  $r_0$  : cavern radius.

or

(If  $k=k(r)$  in the Disturbed zone)

$$\frac{1}{2} \eta_s(T) \left( \frac{3}{n} \right)^n \left( \frac{\sigma_0 - P_1}{2\sigma_n} \right)^n = \frac{1}{\eta} \frac{P_1 - P_0}{r_0^2} \int_{r_0}^{r_e} \frac{dr}{k(r) r^2}$$

$r_e - r_0$  : Disturbed zone thick.

Regarding the experimental results obtained at the WIPP site (Stormont *et al.*, 1991), the following relationship  $k(r) = k(r_0) \left( \frac{r}{r_0} \right)^\alpha$  (with  $\alpha \approx -20$ ) can be considered for the permeability expression.

The results show that long term evolution of the storage is sensitive to the permeability, even very small non measurable (smaller than  $10^{-22} \text{ m}^2$ ) (figure 12).

On the other hand :

- The higher the permeability value, the more the equilibrium pressure  $P_1$  tends towards the initial pore pressure  $P_0$ . Reciprocally, the lower the permeability, the more the equilibrium pressure  $P_1$  tends towards the initial lithostatic pressure  $\sigma_0$ .

- The equilibrium pressure  $P_1$  is more sensitive to permeability in the small caverns (small radius and volume) at a shallow depth.
- For a given permeability value, the higher the exponent  $n$  (of the creep law) and salt fluidity  $\eta_s$ , the higher the equilibrium pressure  $P_1$ .
- In presence of a disturbed zone, the equilibrium pressure  $P_1$  tends towards the initial pore pressure  $P_0$ , when the permeability at the cavern wall  $k_0$  is high (at constant external radius  $r_e$ ) or when the extent of the disturbed zone is significant (i.e. the parameter  $r_e$  increases at constant  $k_0$ ).

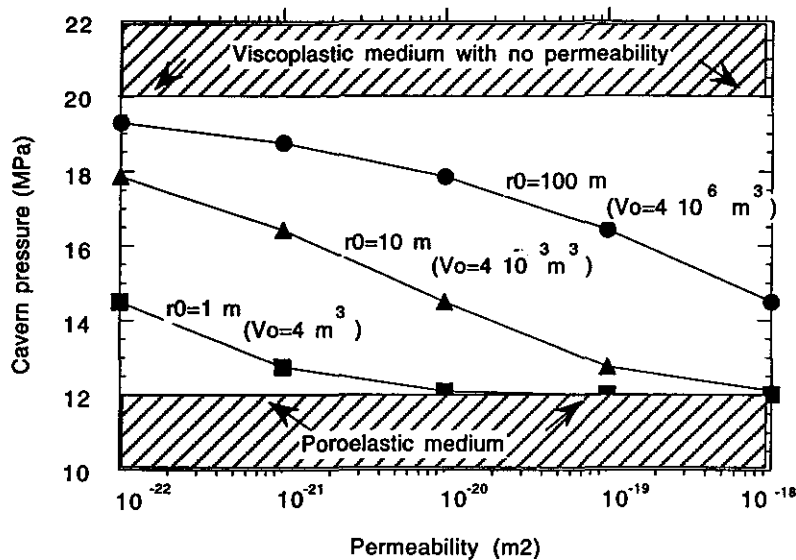


Figure 12. Fluid pressure in the cavern at a steady state for different values of permeability (Depth : 1000 m; Initial pore pressure : 12 MPa; Geostatic pressure : 20 MPa;  $r_0$  : cavern radius).

## CONCLUSION

Based on the experimental results and the theoretical analyses, the following conclusions were obtained :

- The performed field experiment confirms that rock salt is permeable to gas and to brine, even relatively far (16 m) from underground openings;
- The measurements provided by the tests performed with brine were interpreted in a satisfactory way by a model based on Darcy's law (intrinsic permeability value of  $2 \cdot 10^{-21} \text{ m}^2$ );
- Interpretation of the measured gas flow rate show that : (a) after brine percolation, the capillary pressure effect is significant, (b) gas migration is not controlled by Darcy's law;

- When the stress state reaches the values leading to a failure initiation of the damaged rock salt, Terzaghi's concept of effective stress can be applied;
- The proposed theoretical framework based on thermodynamics of open and reactive porous media allows to take into account coupled effects occurring in underground facilities in rock salt;
- The elaborated model shows that "healing" process of damaged salt is partially controlled by mass transfer from grain boundaries to microcracks. This can explain the extremely low permeability of rock salt at a geological time-scale;
- A very low permeability which may not be measurable using present technology (permeability lower than  $10^{-22}$  m<sup>2</sup>) has a significant influence on the long term evolution of a disposal in a saline formation.

**Acknowledgements** - This research was supported by European Commission and the Agence Nationale pour la gestion des Déchets Radioactifs (A.N.D.R.A.). The author expresses his gratitude to these organizations.

#### **PARTIAL REFERENCES**

**A.T.G. (Association Technique de l'industrie du Gaz en France) (1986)**, *Manuel pour le Transport et la distribution du gaz, Stockages Souterrains de Gaz*, Tome XIII, Paris.

**BRODSKY N.S., MUNSON D.E. (1991)**, *The effect of brine on the creep of W.I.P.P. salt in laboratory tests*, In : Rock Mechanics as a multidisciplinary science. Proc. of the 32<sup>nd</sup> US Symposium on Rock Mechanics, J.C. Roegiers. (Ed.) PP 703-712, Balkema.

**COSENZA Ph., GHOREYCHI M. (1993)**, *Coupling between mechanical behavior and transfer phenomena in salt* - In : Proc. of the 3<sup>rd</sup> Conference on Mechanical Behavior of Salt, M. Ghoreychi, P. Bérest, H Hardy, M. Langer. (Eds.) PP 286-307, Trans Tech Publications, Clausthal, ISBN 0-87849-100-7.

**COUSSY O. (1991)**, *Mécanique des Milieux Poreux*, Ed. Technip, 437 p.

**KAZAN Y. GHOREYCHI M., (1996)** *Thermo-mechanical Study of the Near Field around a Storage Borehole in Salt Formations*. European Commission, Official Publications of the European Communities, Luxembourg ; EUR 16946. (In French).

**LANGER M.** (1981), The rheological behavior of rock salt. *Proc. 1st Conf. on Mech. Behavior of Salt*, Penn-State University, pp. 201-231, Trans Tech Publications, Clausthal-Zellerfeld, Germany .

**Mc TIGUE D. F.** (1986), *Thermoelastic response of fluid-saturated porous rock*, J. Geophys. Res., 91, 9533-9542.

**MUNSON D.E., DAWSON P.R. LANGER M.** (1981), The rheological behavior of rock salt. *Proc. 1st Conf. on Mech. Behavior of Salt*, Penn-State University, pp. 201-231, Trans Tech Publications, Clausthal-Zellerfeld, Germany ., Salt constitutive modelling using mechanism map. *Proc. 1st Conf. on Mech. Behavior of Salt*, Penn-State University, 201-231, Trans Tech Publications, Clausthal-Zellerfeld, Germany.

**OLIVELLA S., GENS A., ALONSO E.E., CARRERA J.** (1992), *Constitutive modelling of porous salt aggregates*, Numerical models in Geomechanics, Pande et Pietruszczak (Eds), PP 179-189, Balkema, Rotterdam.

**PEACH C.** (1991), *Influence of deformation on the fluid transport properties of salt rocks*, Thèse de l'université d'Utrecht, Geologica Ultraiectina, N°77, Hollande, ISBN 0072-1026 n°77.

**POUYA A.**, Comportement rhéologique du sel gemme. Application à l'étude des excavations souterraines, Ph. D. Thesis Ecole Nationale des Ponts et Chaussées, Paris, (1991)

**SCHULZE O.** (1991), *Effect of humidity on creep of rocksalt*. Proc. 7<sup>th</sup> Int. Cong. Rock Mechanics, Aachen, Balkema.

**SPIERS C.J., SCHUTJEN P.M.T., BRZESOWSKY R.H., PEACH C.J. ZWART H.J.** (1990), *Experimental determination of constitutive parameters governing creep of rock salt by pressure solution*, Deformation Mechanisms, Rheology and Tectonics, Knipe, R.J. and Rutter E.H (Eds.) N°54, 215-227, Geological Society Spec. Publication, London.

**STORMONT J.C., HOWARD C.L., DAEMEN J.J.K.** (1991), *Changes in rock salt permeability due to nearby excavation*, Rock Mechanics as a Multidisciplinary Science, Roeggiers (Ed.), PP 899-907, Rotterdam.

**STORMONT J. C.** (1997); Discontinuous behaviour near excavations in a bedded salt formation, *Int. J. Mining Geol. Eng.*, 8, 35-56

**THOREL L., GHOREYCHI M.** (1993), *Rock salt damage - Experiment results and interpretation*, In : Proc. of the 3<sup>rd</sup> Conference on Mechanical Behavior of Salt, M. Ghoreychi, P. Bérest, H Hardy, M. Langer. (Eds.) PP 175-190, Trans Tech Publications, Clausthal, ISBN 0-87849-100-7.

**THOREL L.** (1994) *Plasticité et endommagement des roches ductiles - Application au sel gemme*. Thèse de l'Ecole des Ponts et Chaussées, Paris.

**WIECZOREK P., ROTHFUCHS T.** (1986), *In situ permeability measurements, in Results of temperature tests 6 in the Asse Mine*, Vol I., Rapport C.E.C. EUR 10827 EN/I.